



Domino synthesis of quinoxaline derivatives using SBA-Pr-NH₂ as a nanoreactor and their spectrophotometric complexation studies with some metals ions

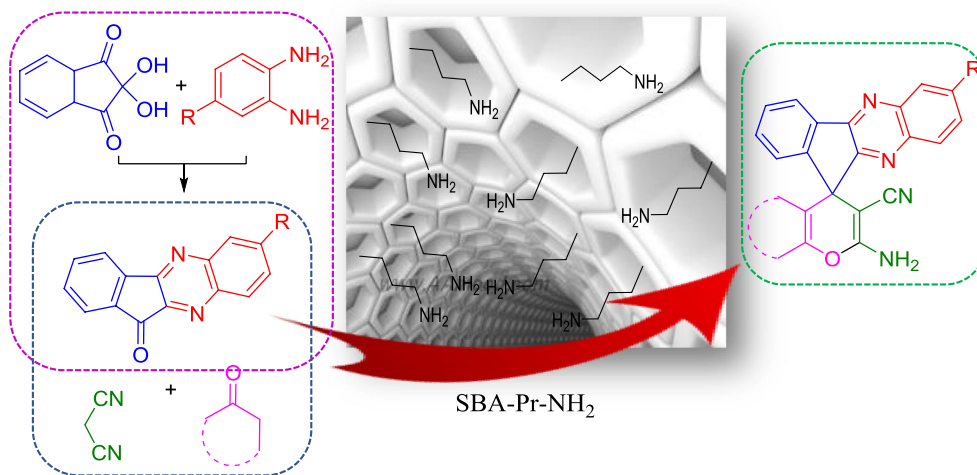
Tahereh Ahmadi¹ · Ghodsi Mohammadi Ziarani¹ · Shahriyar Bahar¹ · Alireza Badiei²

Received: 6 September 2017 / Accepted: 21 January 2018 / Published online: 1 February 2018
© Iranian Chemical Society 2018

Abstract

Amino-functionalized SBA-15 (SBA-Pr-NH₂) with a pore size of 6 nm has been used as a basic nanocatalyst in the domino one-pot synthesis of quinoxaline derivatives via the four-component reaction of ninhydrin, 1,2-aryl-diamines, malono derivatives, and α -methylene carbonyl compound using microwave irradiation. The solid basic catalyst plays a significant role in catalysis, and enhancing the rate and yield of the reaction, it can be easily handled and removed from the reaction mixture by simple filtration and also reused several times without substantial loss of reactivity. Moreover, the complexation reaction between quinoxaline as a model ligand and some metal ions including Cd²⁺, Co²⁺, Cu²⁺, Fe³⁺, Hg²⁺, Ni²⁺, Pb²⁺, and Zn²⁺ ions was examined spectrophotometrically in DMF solution at 25 °C. The formation constants of the resulting complexes were calculated from the computer fitting of the molar absorbance measurements in different mole ratios. The obtained data indicated that the stability constant of the resulting complexes varied in the following order Pb²⁺ > Hg²⁺ > Cd²⁺ > Ni²⁺ > Cu²⁺ > Fe³⁺ > Zn²⁺ > Co²⁺.

Graphical Abstract



Keywords SBA-Pr-NH₂ · Quinoxaline derivatives · Ninhydrin · 1,2-aryl-diamines · Malono derivatives · α -Methylenecarbonyl compound · Microwave irradiation · Four-component domino reaction · Spectrophotometric complexation

✉ Ghodsi Mohammadi Ziarani
gmziarani@hotmail.com; gmohammadi@alzahra.ac.ir

Extended author information available on the last page of the article

Introduction

Functionalized quinoxalines are very important heterocycle compounds, which is a building block of many useful intermediates in organic synthesis and useful dyes [1]. Also they attracted scientists because of their pharmaceutical properties including as antibacterial [2], antiviral [3], as kinase inhibitors [4], and anticancer [5]. Besides clinical drugs and dye applications, quinoxaline compounds have been known as the framework in the preparation of organic semiconductors [6]. Development of many strategies for the preparation of substituted quinoxalines has been reported [7, 8]. The most common methods are the condensation of an α,β -aryl-diamine with a α,β -dicarbonyl compound in refluxing acetic acid or ethanol [9].

Multicomponent reactions (MCRs) have gained significant importance as a tool for the synthesis of a wide variety of useful compounds. Over the past decades, multicomponent reactions have proved to be very powerful and efficient bond-forming tools in organic chemistry [10, 11] and the number of used catalysts to promote this reaction is large such as nanoparticles [12], magnetic nanoparticles [13, 14], and nanoreactors [15, 16]. Magnetic nanoparticles and nanoreactors can be also used as carrier [17–19].

A nanoreactor is a nanoscale environment that a reaction takes place. Due to the nanoscopic confinement effect of the nanoreactor, the physical properties such as density, viscosity, and solubility could be varied, and the chemical properties of reactants and catalysts could be modulated [20]. Several types of nanoreactors have been developed up to now, including carbon nanotubes (CNT) [21, 22], metal–organic frameworks (MOF) [23], zeolites [24], and mesoporous silica [25, 26]. Higher reactivity and selectivity were revealed when reactions were conducted in nanoreactors [27, 28]. Among these nanoreactors, mesoporous silicas, especially SBA-15, have been widely investigated thanks to their controllable size, composition, and morphology, which are highly desirable for catalytic applications. SBA-15 is mesoporous silica, which was synthesized by Zhao and co-workers, firstly [29, 30]. This mesoporous silica is hexagonal nanoporous silica with high surface area, large pore size, remarkable thermal stability, and easily handled and removed from the reaction mixture [31–33]. The surface of SBA-15 can be modified by different functional groups such as organic acids and amines [34]. SBA-Pr-NH₂ can act as an efficient heterogenous solid base catalyst in the organic synthesis. In continuation of our researches [35–39], we used amino-functionalized SBA-15 (SBA-Pr-NH₂) as a heterogeneous nanoreactor in the synthesis of quinoxaline derivatives through the four-component domino reaction of ninhydrin, 1,2-aryl-diamines, malononitrile, and α -methylencarbonyl compound. In 2015, the advances in the use of ninhydrin

in the synthesis of heterocyclic compounds have been published [40].

Experimental

Materials and instruments

The chemical materials which were employed in this work were obtained from Merck Company and used with no purification. Melting points were measured by capillary tube method with an Electrothermal 9200 apparatus. Infrared (IR) spectra were recorded from KBr disks employing a Fourier-transform (FT)-IR Bruker Tensor twenty-seven instrument. ¹H NMR (250 MHz) and ¹³C NMR (62.9 MHz) spectra were run on a Bruker DPX using tetramethylsilane (TMS) as internal standard in DMSO. The X-ray powder diffraction (XRD) pattern of the prepared SBA-Pr-NH₂ nanoreactor was collected by a Philips X'pert MPD diffractometer using Cu K α radiation ($\lambda = 0.15478$ nm). Transmission electron microscopy (TEM) was carried out on a Tecnai G² F30 at 300 kV. All UV–Vis spectra and absorption measurements were recorded on a computerized Specord S 600 Analytik Jena UV–Vis spectrophotometer equipped with a peltier element with a heating rate of 0.1 °C/min to control the temperature.

Synthesis and functionalization of SBA-15

The nanoporous compound SBA-15 was synthesized and functionalized according to our previous report, and the modified SBA-Pr-NH₂ was used as a nanoporous solid basic catalyst in the following reaction [37].

General procedure for the synthesis of spiro[indeno[2,1-b]quinoxaline derivatives

SBA-Pr-NH₂ (0.02 g) was activated into a round-bottomed flask containing a magnetic stirrer at 100 °C for removal of the adsorbed water. The mixture of ninhydrin (1 mmol, 0.178 g), 1,2-aryl-diamines (1 mmol), and SBA-Pr-NH₂ in 5 ml ethanol was heated and stirred at 60 °C to form indenoquinoxalineA; then, after about 5 min, malono derivatives (1 mmol) and α -methylencarbonyl compounds (1 mmol) were added to the mixture of reaction for the synthesis of spiro[indeno[2,1-b]quinoxaline derivatives under reflux condition using MW irradiation (400 W, 80 °C). Completion of the reaction was monitored by TLC. After that, obtained precipitate was cooled to room temperature and extracted from the solvent. Subsequently, the precipitate was dissolved in minimum volume of hot acetone and the unsoluble SBA-Pr-NH₂ catalyst was removed by filtration. The residue was purified by recrystallization from ethanol. The

new compound was characterized by mass, IR, and NMR spectroscopy techniques. The melting points of the products were compared with those reported in the literature.

6'-Amino-3'-phenyl-1'H-spiro[indeno[1,2-b]quinoxaline-1,4'-pyrano[2,3-c]pyrazole]-5'-carbonitrile (5 g)

FT-IR (KBr) ν_{\max} : 3332, 3309, 3239, 3170, 2200, 1658, 1604, and 1405 cm^{-1} . ^1H NMR (250 MHz, $\text{DMSO}-d_6$) δ_{H} : 6.26–6.99 (3H, m, Ar-H), 7.29 (s, 2H, NH_2), 6.50–8.06 (13H, m, Ar-H), 12.84 (s, 1H, NH) ppm. ^{13}C NMR (62.5 MHz, $\text{DMSO}-d_6$) δ_{C} : 48.11, 57.93, 97.34, 119.06, 122.01, 126.07, 127.52, 128.28, 128.51, 129.06, 129.30, 129.49, 129.93, 130.66, 133.25, 136.16, 139.31, 141.56, 142.32, 152.35, 153.55, 156.38, 162.36, 165.20 ppm. MS (m/z , %): 440($[\text{M}^+$], 26), 414(100), 374(22), 280(78), 216(4), 160(22), 66(11).

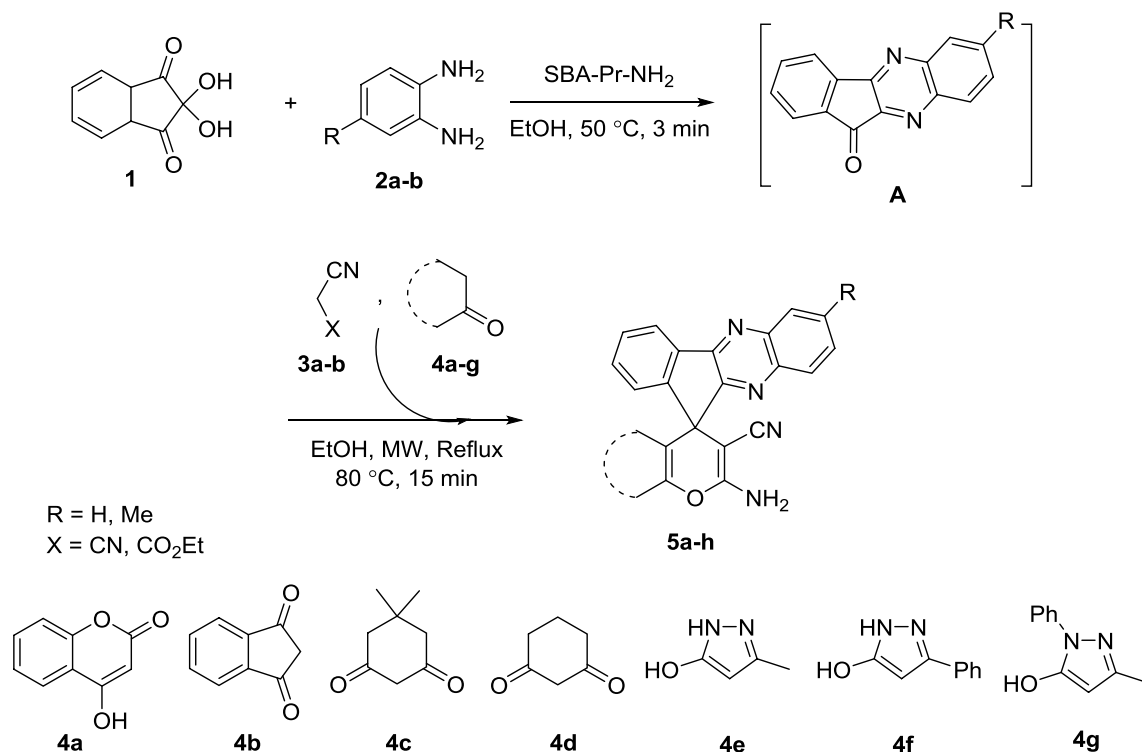
Assessment of mole ratio and formation constants of quinoxaline complexes

In order to calculate the stoichiometry of the resulting complexes of quinoxaline as a model, ligand with some metal ions, spectrophotometric titration was used. For this purpose, 2.5 mL of quinoxaline solution ($5.0 \times 10^{-5} \text{ mol L}^{-1}$) in DMF was located in the spectrophotometer cuvette and the absorbance of solution was measured. Afterward, a suitable

amount of the $10^{-3} \text{ mol L}^{-1}$ solution of different metal ions was added in a stepwise manner using a micro-syringe. Following each addition, the absorbance value of the solution was measured. The addition of metal ions solution was continued until the preferred metal ion to ligand mole ratio was achieved. In the following, the formation constant (k_f) of the obtained complexes between quinoxaline and several metal ions at constant temperature (25°C) was computed by fitting the observed absorbance, A_{obs} , at various metal ion/ligand mole ratios to the equation that previously derived with Shamsipur et al. [41, 42], which expresses the observed electronic absorbance as a function of the free and complexed metal ions and the formation constant assessment from a nonlinear least-squares program KINFIT [43].

Results and discussion

In this method, a rapid and highly efficient strategy for the synthesis of spiro [indeno[1,2-*b*] quinoxaline derivatives **5a–h** through four-component domino condensation reaction of ninhydrin **1**, 1,2-aryl-diamines **2a–b**, malono derivatives **3a–b**, and α -methylencarbonyl compounds **4a–g** in the presence of SBA-Pr- NH_2 under MW irradiation in ethanol was studied (Scheme 1). In order to assess the impact of solvent on the reaction, its progress in different conditions such as reflux in EtOH and solvent-free systems in the presence of



Scheme 1 Synthesis of quinoxaline derivatives **5** using SBA-Pr- NH_2

SBA-Pr-NH₂ was compared and reported in Table 1. The reaction times and yields of the products under various conditions (i.e., reflux, 140 °C, and MW irradiation), in the presence of solvent and under a solvent-free system, were compared, and the best result was obtained after 15 min under MW irradiation in EtOH as solvent (entry 5). We also tested the reaction with various catalysts, and the results showed that SBA-Pr-NH₂ plays a significant role in this reaction and enhances the rate and yield of the reaction. With the optimized reaction conditions, we explored the generality of this method using different 1,2-aryl-diamine, malono derivatives and α -methylcarbonyl compounds. Consequently, according to the current synthetic requirements, this multicomponent procedure under MW irradiation in EtOH and in the optimum quantity of SBA-Pr-NH₂ (0.02 g) is preferable due to the shorter reaction time and high yields of the products. The new products were characterized by melting point, IR, ¹H NMR, ¹³C NMR spectra, and MS spectral analysis. Melting points of known products were compared with reported values in the literature (Table 2).

The suggested reaction mechanism and significant role of SBA-Pr-NH₂ as solid basic catalyst in accelerating reaction rate are depicted in Scheme 2. First, through a nucleophilic addition of 1,2-aryl-diamine moiety to ninhydrin **1**, indenoquinoxaline **A** was achieved. Deprotonation of malononitrile

by SBA-Pr-NH₂ followed by Knoevenagel condensation of indenoquinoxaline **A** with malononitrile **3** afforded intermediate **B**, which subsequently underwent Michael addition with α -methylene carbonyl compound **4** to form intermediate **C**. In the next step, the oxygen of the enolate attacks to the nitrile group in intermediate **C** and the desired products were obtained after a cyclization.

There are only few reports for spiro[indeno[1,2-*b*]quinoxaline-11,4'-pyrano-5'-carbonitriles synthesis through the mentioned four-component domino reaction in the literature. As shown in Table 3, the products were synthesized with excellent yields and short reaction times when compared with other existing methods.

Spectrophotometric studies

The absorption spectra of quinoxaline and its Cd²⁺, Co²⁺, Cu²⁺, Fe³⁺, Hg²⁺, Ni²⁺, Pb²⁺, and Zn²⁺ complexes in DMF solution are shown in Fig. 1. As can be seen, the spectral changes (increase in the absorbance in the 350 nm) are the result of the complex formation between quinoxaline and metal cations. The stoichiometry of the obtained complexes with different metal ions was measured by the mole ratio method, and the resultant plots of the absorbance change versus the metal ion/quinoxaline mole ratio at 350 nm

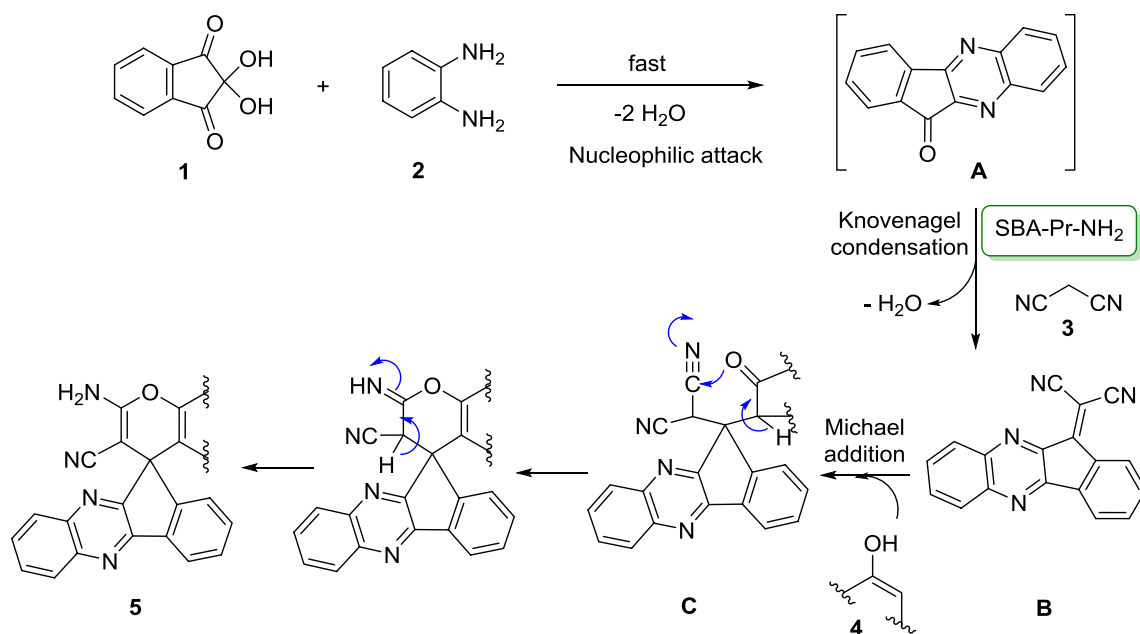
Table 1 Optimization of reaction condition^a for the synthesis of quinoxaline **5e**

| Entry | Catalyst | Reaction condition | Temperature (°C) | Time (min) | Yield ^a (%) |
|-------|--------------------------------------------------|--------------------|------------------|------------|------------------------|
| 1 | AcONH ₄ | EtOH, Reflux | 80 | 12 h | 80 |
| 2 | SBA-Pr-SO ₃ H | EtOH, Reflux | 80 | 8 h | Trace |
| 3 | SBA-Pr-SO ₃ H | EtOH, MW | 80 | 20 | Trace |
| 4 | SBA-Pr-NH ₂ | EtOH, Rele 3flux | 80 | 7 h | 85 |
| 5 | SBA-Pr-NH ₂ | EtOH, MW | 80 | 15 | 94 |
| 6 | SBA-Pr-NH ₂ /SBA-Pr-SO ₃ H | EtOH, MW | 80 | 15 | 94 |
| 7 | SBA-Pr-NH ₂ | Neat | 170 | 60 | 80 |
| 8 | SBA-Pr-NH ₂ | Neat | 120 | 4 h | 50 |

^aNinhydrin (1 mmol), *o*-phenyldiamine (1 mmol), malononitrile (1 mmol), 3-methyl-5-pyrazolone (1 mmol), and catalyst

Table 2 Synthesis of quinoxaline derivatives in the presence of SBA-Pr-NH₂

| Entry | R | X | Carbonyl compound | Product | Yield (%) | M.p. (°C) | M.p. (Lit.) |
|-------|----|--------------------|-------------------|---------|-----------|-----------|---------------|
| 1 | H | CN | 4a | 5a | 90 | 298 dec. | 297 dec. [44] |
| 2 | H | CO ₂ Et | 4b | 5b | 88 | 290 dec. | 289 dec. [44] |
| 3 | H | CN | 4c | 5c | 93 | 282 dec. | 280 dec. [44] |
| 4 | H | CN | 4d | 5d | 92 | 276 dec. | 278 dec. [44] |
| 5 | H | CN | 4e | 5e | 94 | 270–272 | 263–266 [45] |
| 6 | Me | CN | 4e | 5f | 89 | 262–264 | 258–262 [45] |
| 7 | H | CN | 4f | 5g | 98 | 275–277 | New |
| 8 | H | CN | 4g | 5h | 95 | 241–243 | 241–244 [45] |



Scheme 2 Proposed mechanism for the synthesis of quinoxaline derivatives **5**

Table 3 Comparison of different conditions in the synthesis of compound **5 h**

| Entry | Catalyst | Solvent | Condition | Time (h) | Yield (%) | References |
|-------|---------------------------------|---------|-----------|----------|-----------|------------|
| 3 | Na ₂ CO ₃ | EtOH | 70 °C | 17 | 85 | [45] |
| 1 | NH ₄ OAc | EtOH | Reflux | 12 | 93 | [46] |
| 2 | InCl ₃ | EtOH | Reflux | 10 | 93 | [44] |
| 4 | SBA-Pr-NH ₂ | EtOH | MW | 15 min | 95 | This work |

Fig. 1 UV–Vis spectra of quinoxaline (5×10^{-5} M) and its Cd²⁺, Co²⁺, Cu²⁺, Fe³⁺, Hg²⁺, Ni²⁺, Pb²⁺, and Zn²⁺ complexes in DMF solution

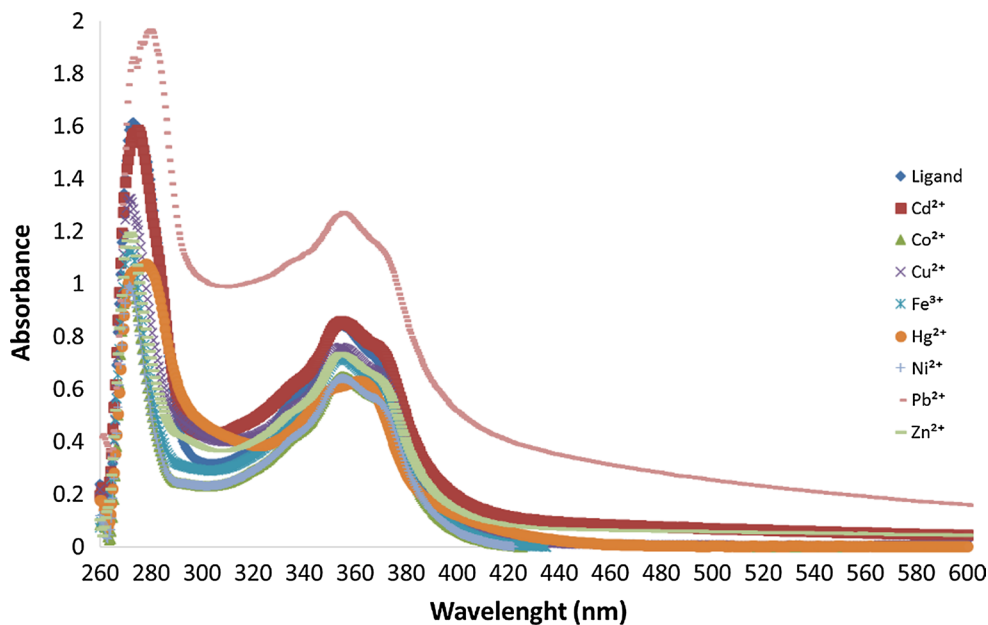


Fig. 2 Mole ratio plots of absorbance as $[M^{n+}]/[L]$ at 350 nm

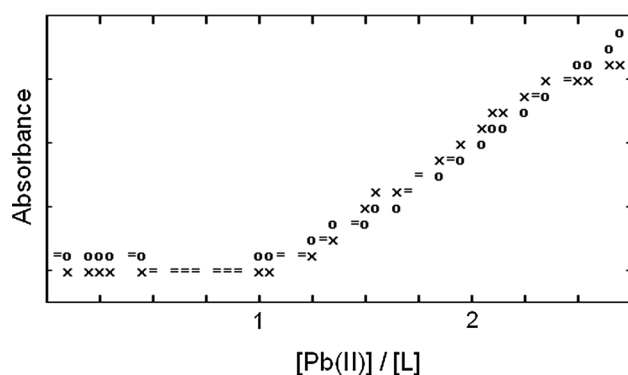
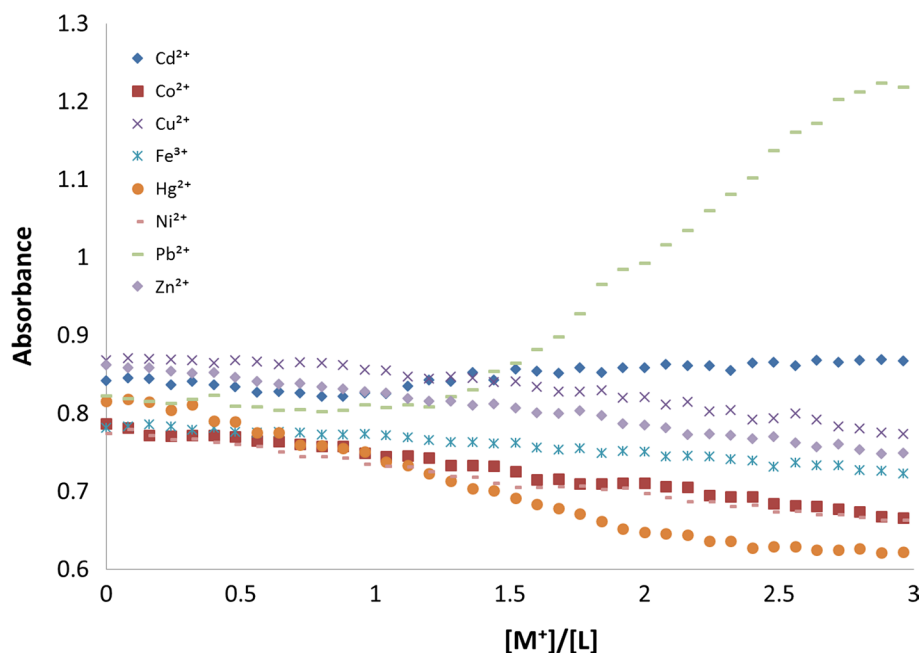


Fig. 3 Computer fitting of absorbance versus $[Pb^{2+}]/[L]$ mole ratio plot in DMF at 25 °C, (x) experimental point, (O) calculated point, (=) experimental and calculated points are the same within the resolution of the plot

are shown in Fig. 2. The stability constants of the formed complexes between different metal ions and quinoxaline were obtained using measurement of the variation in the absorbance amount of the solutions in which different concentrations of metal ions were added to constant quantity ($5 \times 10^{-5} \text{ mol L}^{-1}$) of quinoxaline solution.

For assessment of the stability constants of the resultant complexes from absorbance amount versus $[M]/[L]$ mole ratio, a nonlinear least-squares curve fitting program KINFIT was applied. A model computer fitting of the absorbance–mole ratio data for the Pb^{2+} ion is illustrated in Fig. 3. The $\log k_f$ values for all metal ions complexes which evaluated from the computer fitting of the related absorbance–mole ratio data at 25 °C are shown in Table 4. The obtained data revealed that, at 25 °C,

Table 4 $\log k_f$ values for various metal ions complexes with quinoxaline

| Metal ion | $\log k_f \pm \text{SD}$ |
|-----------|--------------------------------|
| Pb^{2+} | $3.87 \pm 1.55 \times 10^{-3}$ |
| Hg^{2+} | $3.72 \pm 2.16 \times 10^{-4}$ |
| Cd^{2+} | $3.03 \pm 1.23 \times 10^{-4}$ |
| Ni^{2+} | $3.02 \pm 1.02 \times 10^{-4}$ |
| Cu^{2+} | $3.00 \pm 7.77 \times 10^{-4}$ |
| Fe^{3+} | $3.00 \pm 5.13 \times 10^{-4}$ |
| Zn^{2+} | $2.99 \pm 7.35 \times 10^{-4}$ |
| Co^{2+} | $2.99 \pm 6.99 \times 10^{-4}$ |

the stabilities of the complexes vary in the accordance $Pb^{2+} > Hg^{2+} > Cd^{2+} > Ni^{2+} > Cu^{2+} > Fe^{3+} > Zn^{2+} > Co^{2+}$.

Synthesis and functionalization of SBA-15

SBA-15 was afforded via triblock copolymer pluronic P126 as a commercially available structure-directing agent [29]. A pathway for the synthesis of SBA-Pr-NH₂ is shown in Fig. 4, and post-grafting technique was used for the modification of SBA-15 surface with the APTES ((3-aminopropyl)triethoxysilane) in refluxing toluene for 24 h [37].

Analysis of the catalyst surface was performed by totally different ways including thermogravimetric analysis (TGA), Brunauer–Emmett–Teller (BET) analysis, X-ray diffraction (XRD), and elemental analysis (CHN). These analyses proved that the 3-aminopropyl groups were successfully immobilized into the pores [37].

In this work, SBA-Pr-NH₂ was used as a nanoporous catalyst in the synthesis of **5**. Figure 5 shows the SEM and TEM images of SBA-Pr-NH₂. The SEM image shows uniform

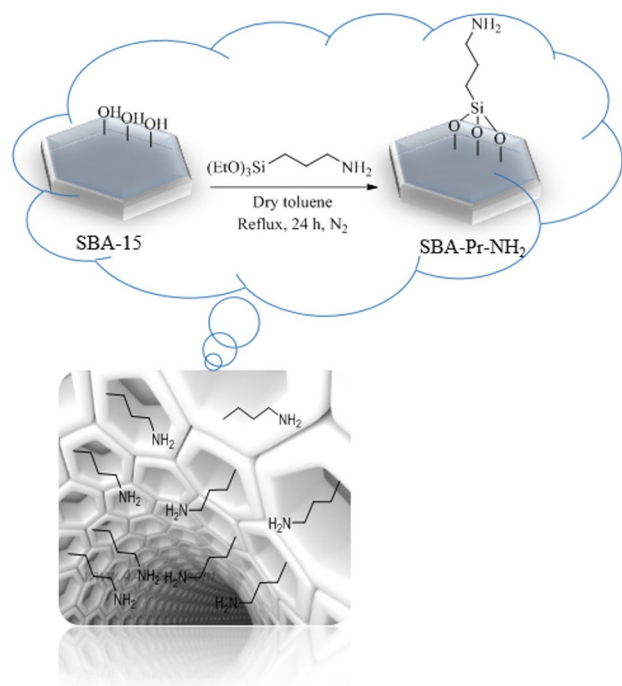
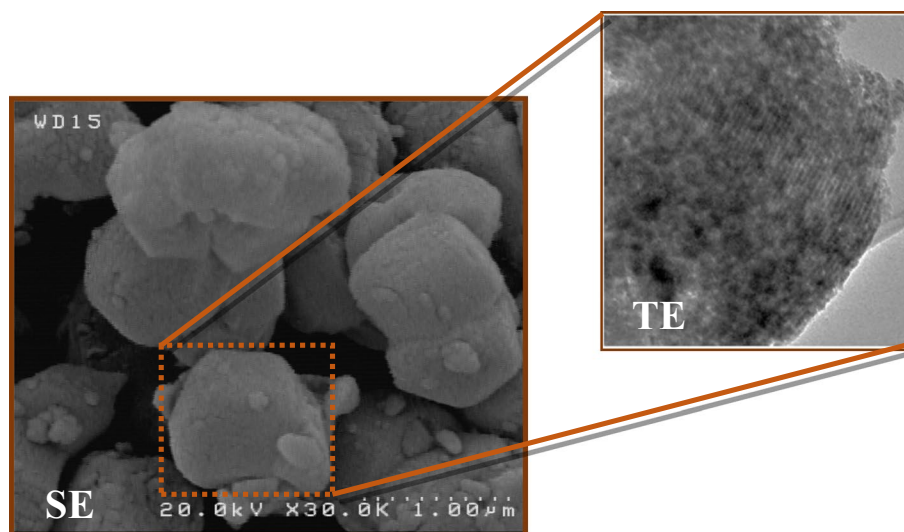


Fig. 4 Preparation of SBA-Pr-NH₂

particles about 1 μm which have the same morphology as SBA-15. It can be illustrated that the morphology of the solid was remained and no changes occurred during the surface modifications. Furthermore, TEM image shows parallel channels in the SBA-Pr-NH₂, which resembled the configuration of the pores in SBA-15.

Fig. 5 SEM and TEM images of SBA-15-NH₂



As depicted in Fig. 6, the XRD patterns of SBA-15 showed the intensity of the strongest reflection peaks at 0.8° – 0.9° with two other relatively intense of less reflections at higher degrees, which might be indexed to the 100, 110, and 200 planes, respectively. NH₂-SBA-15 was also described by a similar pattern, informing the successful grafting of APTES into the channels of the mesostructure without changing the structural integrity of SBA-15 [47].

As shown in Fig. 7, the prepared SBA-15-NH₂ has the amine groups within its pores. As the pore size of the catalyst is about 6 nm, which was proved by BET analysis, the starting materials enter into the pores and react together in contact with the basic groups to give the product. Therefore, SBA-15-NH₂ is a solid basic catalyst, which can act as a nontoxic, available, and reusable nanoreactor.

At the end of reaction, the reusability of the catalyst was determined for the preparation of compounds **5e**. As shown in Fig. 8, the catalyst can be recovered and reused four times without significant loss of activity. The yields for the four runs were 91, 88, 86, and 83%, respectively.

Conclusion

In the present work, SBA-Pr-NH₂ organocatalyst was prepared and well characterized. The prepared SBA-Pr-NH₂ nanoparticles play a significant role in the domino four-component reaction of ninhydrin, 1,2-aryl-diamines, malono compounds, and α -methylene carbonyl for the synthesis of spiro[indeno[2,1-*b*]quinoxaline derivatives. The key advantages of this study include high yields, short reaction times,

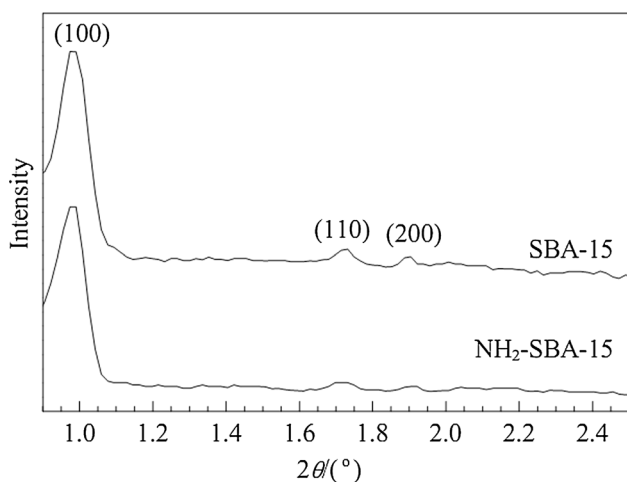


Fig. 6 Low-angle XRD patterns of SBA-15 and SBA-Pr-NH₂

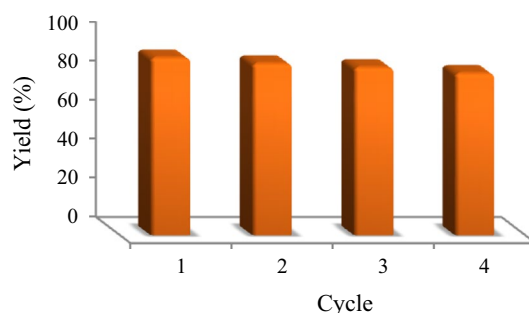


Fig. 8 Reusability of SBA-Pr-NH₂ in the synthesis of compound 5e

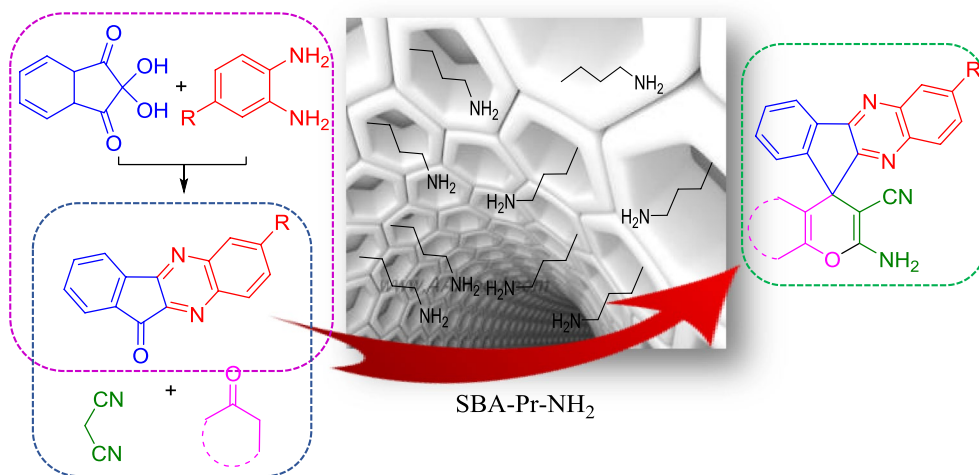


Fig. 7 SBA-15-NH₂ acts as a nanoreactor

easy workup, available catalyst, reusable catalyst, and purification of compounds using a crystallization method (non-chromatographic). In the following, the complexation study of the quinoxaline with some metal ions indicated that the prepared compound has a good selectivity for the complexation of the Pb²⁺ ions. The obtained $\log k_f$ values for all metal ions complexes from the computer fitting of the related absorbance–mole ratio data indicated that the stabilities of the complexes vary in the accordance Pb²⁺ > Hg²⁺ > Cd²⁺ > Ni²⁺ > Cu²⁺ > Fe³⁺ > Zn²⁺ > Co²⁺.

Acknowledgements We gratefully acknowledge the financial support from the Research Council of Alzahra University and the University of Tehran. This work was supported by the Iran National Science Foundation (INSF) under Contract 95005360.

References

1. E. Brock, D. Lewis, T. Yousaf, H. Harper, "The Procter & Gamble Company", USA WO 9951688, A1 (1999)
2. L.E. Seitz, W.J. Suling, R.C. Reynolds, J. Med. Chem. **45**, 5604 (2002)

3. M. Loriga, S. Piras, P. Sanna, G. Paglietti, *Farmacol. Sci.* **52**, 157 (1997)
4. W. He, M.R. Myers, B. Hanney, A.P. Spada, G. Bilder, H. Galzcin-ski, D. Amin, S. Needle, K. Page, Z. Jayyosi, *Bioorganic Med. Chem. Lett.* **13**, 3097 (2003)
5. C.W. Lindsley, Z. Zhao, W.H. Leister, R.G. Robinson, S.F. Bar-nett, D. Defeo-Jones, R.E. Jones, G.D. Hartman, J.R. Huff, H.E. Huber, *Bioorganic Med. Chem. Lett.* **15**, 761 (2005)
6. S. Dailey, W.J. Feast, R.J. Peace, I.C. Sage, S. Till, E.L. Wood, *J. Mater. Chem.* **11**, 2238 (2001)
7. G.H. Woo, J.K. Snyder, Z.-K. Wan, *Prog. Heterocycl. Chem.* **14**, 279 (2002)
8. A. Porter, A. Katritzky, C. Rees, *Comprehensive Heterocyclic Chemistry*, vol. 3, ed. by A.R. Katritzky, C.W. Ress (Pergamon Press, Oxford, 1984)
9. D.J. Brown, E.C. Taylor, J.A. Ellman, *The Chemistry of Hetero-cyclic Compounds, Quinoxalines: Supplement II*, vol. 61 (Wiley, Hoboken, 2004)
10. T. Ahmadi, G. Mohammadi Ziarani, P. Gholamzadeh, H. Mol-labagher, *Tetrahedron Asymmetry* **28**, 708 (2017)
11. Z. Zareai, M. Khoobi, A. Ramazani, A. Foroumadi, A. Souldozi, K. Ślepokura, T. Lis, A. Shafiee, *Tetrahedron* **68**, 6721 (2012)
12. A. Ramazani, P.A. Asiabi, H. Aghahosseini, F. Gouranlou, *Curr. Org. Chem.* **21**, 908 (2017)
13. H. Aghahosseini, A. Ramazani, K. Ślepokura, T. Lis, *J. Colloid Interface Sci.* **511**, 222 (2018)
14. S.T. Fardood, A. Ramazani, S. Moradi, *J. Sol-Gel. Sci. Technol.* **82**, 432 (2017)
15. V. Fathi Vavsari, G. Mohammadi Ziarani, A. Badiei, S. Balalaie, *J. Iran. Chem. Soc.* **13**, 1037 (2016)
16. G. Mohammadi Ziarani, L. Seyedakbari, S. Asadi, A. Badiei, M. Yadavi, *Res. Chem. Intermed.* **42**, 499 (2016)
17. R. Tarasi, M. Khoobi, H. Niknejad, A. Ramazani, L. Ma'mani, S. Bahadorikhalili, A. Shafiee, *J. Magn. Magn. Mater.* **417**, 451 (2016)
18. A. Mashhadi, A. Malekzadeh, S.J. Ramazani, J. Tabatabaei Rezaei, H. Niknejad, *J. Colloid Interface Sci.* **490**, 64 (2017)
19. V. Fathi Vavsari, G. Mohammadi Ziarani, A. Badiei, *RSC Adv* **5**, 91686 (2015)
20. H. Aghahosseini, A. Ramazani, F. Gouranlou, S. Woo Joo, *Curr. Org. Synth.* **14**, 810 (2017)
21. X. Pan, Z. Fan, W. Chen, Y. Ding, H. Luo, X. Bao, *Nat. Mater.* **6**, 507 (2007)
22. P. Serp, E. Castillejos, *Chem Cat Chem* **2**, 41 (2010)
23. C.-D. Wu, A. Hu, L. Zhang, W. Lin, *J. Am. Chem. Soc.* **127**, 8940 (2005)
24. S. Mandal, D. Roy, R.V. Chaudhari, M. Sastry, *Chem. Mater.* **16**, 3714 (2004)
25. G. Mohammadi Ziarani, N. Lashgari, A. Badiei, *J. Mol. Catal. A: Chem.* **397**, 166 (2015)
26. A. Badiei, H. Goldoos, G. Mohammadi, Ziarani, *Appl. Surf. Sci.* **257**, 4912 (2011)
27. Z. Chen, Z. Guan, M. Li, Q. Yang, C. Li, *Angew. Chem. Int. Ed.* **50**, 4913 (2011)
28. B.K. Ghosh, S. Hazra, B. Naik, N.N. Ghosh, *J. Nanosci. Nano-technol.* **15**, 6516 (2015)
29. D. Zhao, J. Feng, Q. Huo, N. Melosh, G.H. Fredrickson, B.F. Chmelka, G.D. Stucky, *Science* **279**, 548 (1998)
30. D. Zhao, Q. Huo, J. Feng, B.F. Chmelka, G.D. Stucky, *J. Am. Chem. Soc.* **120**, 6024 (1998)
31. P. Gholamzadeh, G. Mohammadi Ziarani, N. Lashgari, A. Badiei, P. Asadiatouei, *J. Mol. Catal. A: Chem.* **391**, 208 (2014)
32. G. Mohammadi Ziarani, N. Lashgari, A. Badiei, *J. Mol. Catal. A: Chem.* **397**, 166 (2015)
33. G. Mohammadi Ziarani, N. Lashgari, A. Badiei, *Curr. Org. Chem.* **21**, 674 (2017)
34. L. Saikia, D. Srinivas, P. Ratnasamy, *Microporous Mesoporous Mater.* **104**, 225 (2007)
35. M. Karimi, A. Badieia, G. Mohammadi Ziarani, *Chem. Pap.* **70**, 1431 (2016)
36. J. Afshani, A. Badiei, N. Lashgari, G. Mohammadi Ziarani, *RSC Adv.* **6**, 5957 (2016)
37. G. Mohammadi Ziarani, N. Mohtasham Hosseini, N. Lashgari, A. Badiei, *Res. Chem. Intermed.* **41**, 7581 (2015)
38. G. Mohammadi Ziarani, F. Nouri, M. Rahimifard, A. Badiei, A. Abolhassani Soorki, *Rev. Roum. Chim.* **60**, 331 (2015)
39. G. Mohammadi Ziarani, Z. Hassanzadeh, P. Gholamzadeh, A. Abolhassani Soorki, *Rev. Roum. Chim.* **61**, 77 (2016)
40. G. Mohammadi Ziarani, N. Lashgari, F. Azimian, H.G. Kruger, P. Gholamzadeha, *ARKIVOC* **6**, 1 (2015)
41. J. Ghasemi, M. Shamsipur, *J. Coord. Chem.* **36**, 183 (1995)
42. H. Khajesharifi, M. Shamsipur, *J. Coord. Chem.* **35**, 289 (1995)
43. J.L. Dye, V.A. Nicely, *J. Chem. Educ.* **48**, 443 (1971)
44. A. Hasaninejad, N. Golzar, A. Zare, *J. Heterocycl. Chem.* **50**, 608 (2013)
45. E. Soleimani, M. Hariri, P. Saei, *C. R. Chim.* **16**, 773 (2013)
46. A. Hasaninejad, N. Golzar, M. Shekouhy, A. Zare, *Helv. Chim. Acta* **94**, 2289 (2011)
47. G. Mohammadi Ziarani, A. Badiei, S. Mousavi, N. Lashgari, A. Shahbazi, *Chin. J. Catal.* **33**, 1832 (2012)

Affiliations

Tahereh Ahmadi¹ · Ghodsi Mohammadi Ziarani¹ · Shahriyar Bahar¹ · Alireza Badiei²

¹ Department of Chemistry, Alzahra University, Vanak Square, Tehran, P.O. Box 1993893973, Iran

² School of Chemistry, College of Science, University of Tehran, Tehran 14155-6455, Iran